photonics

MDPI

Article

Real-Time Chlorophyll-a Pigment Monitoring of *Chlamydomonas reinhardtii* in a Controlled Environment Using Pulsed LED Fluorescence LiDAR System

Jumar G. Cadondon [1,2,*], Edgar A. Vallar [1], Tatsuo Shiina [3] and Maria Cecilia D. Galvez [1]

[1] Environment and Remote Sensing Research (EARTH) Laboratory, Physics Department, College of Science, De La Salle University Manila, 2401 Taft Avenue, Manila 0922, Philippines
[2] Division of Physical Sciences and Mathematics, College of Arts and Sciences, University of the Philippines Visayas-Miagao Campus, Miagao 5023, Philippines
[3] Graduate School of Engineering, Chiba University, Yayoi-cho, Chiba-shi 263-8522, Japan
* Correspondence: jumar_cadondon@dlsu.edu.ph

Abstract: The real-time chlorophyll-a pigment monitoring of *C. reinhardtii* is studied using our developed LED fluorescence light detection and ranging (LiDAR) system. It features a portable set-up that uses a pulsed LED module with an excitation wavelength of 385 nm. We were able to monitor the different growth phases of *C. reinhardtii* with specific cultivation parameters. The developed fluorescence LiDAR system showed the linear correlation of its chlorophyll-a signal with the optical density and EEM fluorescence measurements at 680 nm emission wavelength. Water quality and weather parameters were also measured, which explains the variation in the growth dynamics of *C. reinhardtii* during the sampling period. The results from the monitoring demonstrated a different technique that can be used in estimating algal biomass in the environment.

Keywords: LED fluorescence LiDAR; optical sensing; remote sensing; chlorophyll-a; *Chlamydomonas reinhardtii*; applied optics

Citation: Cadondon, J.G.; Vallar, E.A.; Shiina, T.; Galvez, M.C.D. Real-Time Chlorophyll-a Pigment Monitoring of *Chlamydomonas reinhardtii* in a Controlled Environment Using Pulsed LED Fluorescence LiDAR System. *Photonics* **2023**, *10*, 144. https://doi.org/10.3390/photonics10020144

Received: 15 December 2022
Revised: 21 January 2023
Accepted: 26 January 2023
Published: 30 January 2023

1. Introduction

Photosynthetic microbes such as algae are commonly used in different sectors [1]. A promising contribution of algal biomass is currently used in foods, which enhances the nutritional value of the product [2]. These added nutrients have proven beneficial to animal and human health, decreasing the incidence of several diseases and/or illnesses [3,4]. In the environment, algae are highly dependent on several parameters, such as temperature, salinity, pH and nutrient content, which may increase or decrease their growth and production [5,6].

There are thousands of microalgae genera; one of the few microalgae targeted for food and commercial production is *Chlamydomonas reinhardtii* [7,8]. *C. reinhardtii* is a freshwater green alga that has been subjected to many genetic studies and can be grown in the laboratory. It is usually used to study phenomena such as photosynthesis, flagella locomotion, and light sensing [6,9]. It has been observed that several environmental parameters affect our natural resources due to changes in land and waters [10,11].

Current methods for measuring algal biomass use dry weight measurements, flow cytometry, spectroscopy, and in situ fluorescence probes [12–17]. These conventional measurements require sample collection and preparation in the environment.

Information can be obtained from the area through remote sensing of the Earth's surface, which is carried out without direct contact [18]. The sensors used in these systems vary, using different sources of energy radiation. The data produced can be collected using seaborne [19,20], airborne [21,22], and spaceborne remote sensing [23,24], which can be used in the assessment of chlorophyll-a and algal biomass. One type of active remote

sensing technique uses a fluorescence light detection and ranging (LiDAR) system. It is defined as a non-invasive, non-contact technique that utilizes laser-induced fluorescence technique on the Earth's surface at varying conditions [25]. Several fluorescence LiDAR systems were used in algal monitoring [26–28], water quality assessment, cultural heritage conservation [25], and the evaluation of plant biodiversity [29]. Several LiDAR systems vary in terms of the optical properties of the receiving and transmitting components. Some fluorescence LiDAR systems have higher overlap, providing a gap in the near-range measurements. Our study fills in the missing data by providing an understanding of the behavior of algae at a closer range [30].

We have previously reported the use of a portable LED fluorescence LiDAR system to measure the chlorophyll-a pigment of Spirulina [28]. This has been used to estimate the chlorophyll-a pigment of a commercialized AZTEC spirulina with varying algal biomass. LED mini LiDAR systems were reported for atmospheric application [30,31] and Mars rover exploration [32]. In this study, the researchers aimed to monitor the chlorophyll-a pigment of *C. reinhardtii* under specific growth conditions. This paper demonstrates the use of the developed fluorescence light detection and sensing system in estimating chlorophyll-a pigment at varying growth phases of an algae. It contributes to the development of a portable environmental monitoring system that can be easily used by the government and private sectors.

2. Experimental Preparation and Detection of *C. reinhardtii*

The LED fluorescence LiDAR set-up was designed for on-site use. In this section, the growth conditions and parameters of *C. reinhardtii* are discussed. Standard methods, such as optical density, excitation-emission matrix fluorescence analysis, and estimated chlorophyll-a measurements, were used for correlation purposes. In this study, the growth phases of *C. reinhardtii*, from the lag phase to the death phase, were recorded using the aforementioned methods.

2.1. C. reinhardtii Sample Preparation and Cultivation Parameters

A 12.5% inoculum of *C. reinhardtii* was prepared with an optical density of 0.3. Three replicates of the inoculum were made. BG-11 (Blue-green 11) medium was used for the *C. reinhardtii* inoculum in this study and a pH value of 8. This is widely used for freshwater algae and protozoa [33]. The resulting measurements are shown in Table 1.

Table 1. BG 11 culture media used in cultivating *C. reinhardtii*..

Compound	Final Concentration (g/L Distilled H_2O)
$NaNO_3$	1.5
K_2HPO4	0.04
$MgSO_4.7H_2O$	0.075
$CaCl_2.2H_2O$	0.036
Citric acid	0.006
$FeSO_4.7H_2O$	0.006
EDTA	0.001
Na_2CO_3A5 micronutrient solution	0.021 mL

The algae were cultured in an 8 L prescribed medium with the 12.5% inoculum. The photoperiod on the growth of algae was set at 12 h/12 h (light/dark cycle).

2.2. LED Fluorescence LiDAR System

The construction and experiments using a biaxial optics fluorescence LiDAR system were conducted outside during nighttime as shown in Figure 1.

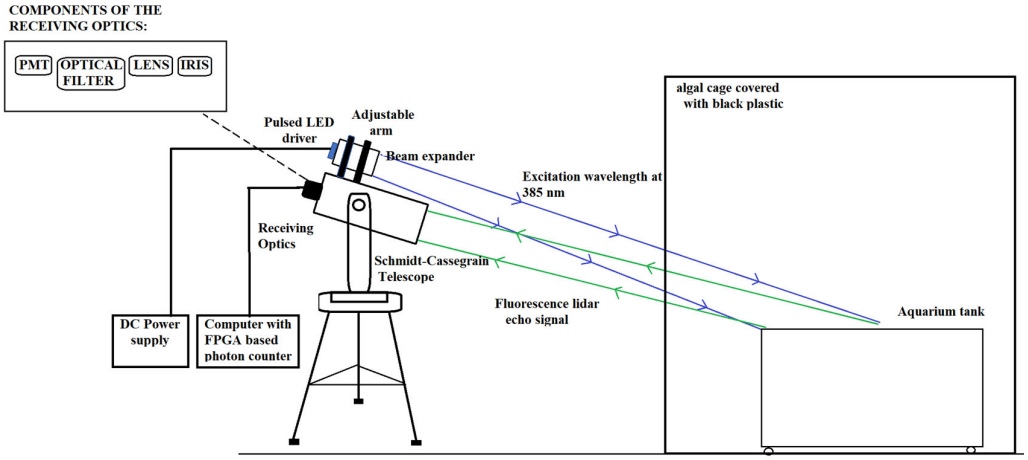

Figure 1. The design of the pulsed LED fluorescence lidar system. The arrow diagram represents the excitation beam from the transmitting component and fluorescence backscatter signal from the algal tank [28].

The transmission of excited light and reception of the backscattered fluorescence signal from the algal sample was conducted using a tabletop Schmidt-Cassegrain Telescope (Kenko Sky Explorer SE-AT90mm, Tokyo, Japan). The eyepiece of the telescope was modified to add the iris, lens, bandpass filter at 680 ± 5 nm (Thorlabs, FB680-10, Newton, NJ, USA), and a photomultiplier tube (Hamamatsu Photonics, R6350P, Hamamatsu, Japan). The tube was designed to detect very weak backscattered signals and was directly connected to a photon-counting board (Trimatiz Co., Ltd., Photon Tracker, Chiba, Japan). It has multiple channel detection features with a system lock of 550 MHz with an approximate power consumption of 2 watts for each channel. A detailed discussion can be read in our previous paper measuring the chlorophyll-a pigment of Spirulina [28]. The receiving and transmitting components of the pulsed LED fluorescence LiDAR system are listed in Table 2.

Table 2. Specifications of the pulsed LED fluorescence LiDAR system.

Transmitter	
LED Name/Brand	Nichia, NCSU034C
Wavelength	385 nm
Peak power	830 mW
Resolution	1.2 m
Bandwidth	10.92 ns
Repetition	500 kHz
Beam diameter	50 mmΦ
Beam divergence	5 mrad
Receiver	
Telescope	Schmidt-Cassegrain
Beam diameter	100 mmΦ
Beam divergence	3 mrad
Bandpass filters: At 680 nm: -Thorlabs (FB680-10)	680 ± 5 nm
Detection device	Photomultiplier tube, Hamamatsu (R6350P)

Table 2. *Cont.*

Photon Counting Board	
Photon Counting Device/Brand	Spartan 6 (FPGA device) Trimatiz Co. Ltd. (Chiba, Japan), Photon tracker
System lock	550 MHz
BIN Width	5 ns (0.75 m)
BIN length	50
Acquisition count	167777214 (max)
Trigger Input Threshold level	300 mV

2.3. Pulsed LED Fluorescence LiDAR Equation

The portable LED fluorescence LiDAR was positioned 5 m away from the algal tank. The design of the algal cage only allows the detection of *C. reinhardtii* and its growth phases from Day 1. Three out of four tanks were covered in a matte blackboard to remove detection from other tanks. The chlorophyll-a concentration of algae has been reported to have linear proportionality with the fluorescence LiDAR signal, as shown by the equation.

$$log\left(E(\lambda_F,\ R)R^2\right) = g(\lambda_F,\ \lambda)C_{algae} \quad (1)$$

where $E(\lambda_F,\ R)R^2$ is the fluorescence lidar signal (in counts·m^2), $g(\lambda_F,\ \lambda)$ is the correlation factor and C_{algae} is the chlorophyll-a concentration (molecule/m^3) observed. The correlation factors are components of the transmitting and receiving systems of the pulsed LED fluorescence LiDAR [28,34]. All other measurements were conducted after the LiDAR experiments.

2.4. Absorbance and EEM Fluorescence Measurements

Each sampling day, 1 mL sample was collected through a cuvette from each algal tank to measure the medium's optical density at 680 nm (OD 680) using a spectrometer setup (Genesis 10uv Thermospectronic, Waltham, MA, USA).

Using EEM images, the growth phases of *C. reinhardtii* for chlorophyll-a measurements can be observed. A fluorescence spectroscopy set-up (Ocean Optics Spectrometer, New York, NY, USA) was assembled for fluorescence measurements of organic matter and algal samples [13,14,28]. From the collected excitation-emission pairs, the excitation region considered is 250 to 450 nm and emission (fluorescence) ranges from 600 to 800 nm. The decomposition and analysis of overlapping spectra found in EEMs were conducted using parallel factor analysis [15].

2.5. Other Parameters Such as Water Quality and Weather Measurements

The light source set-up was designed so that it can be easily removed when conducting the LiDAR and standard measurements. Four linear fluorescent lamps with a total light concentration of 4800 lux or 648 µmol m^{-2} s^{-1} were used for artificial sunlight. They were controlled with a timer set under 12 h/12 h light–dark conditions in the aquarium tank. An aerator pump was installed to provide the necessary amount of carbon dioxide for photosynthesis [35,36].

Water quality parameters were also measured, such as pH, water temperature and electrical conductivity, using a portable field monitoring device (Hach HQ40D/intelliCAL, Loveland, CO, USA). A local weather station (Davis Vantage Pro 2, Davis Instruments, Hayward, CA, USA) was stationed in the building to measure environmental parameters such as relative humidity and temperature.

3. Results

3.1. Pulsed LED Fluorescence LiDAR Signal of C. reinhardtii

Necessary calibrations and adjustments of the fluorescence LiDAR instrument were conducted. The in situ remote sensing of *C. reinhardtii* at nighttime was performed at cultivation parameters. The fluorescence signal measurements of *C. reinhardtii* are dependent on the components of the constructed fluorescence LiDAR system. Real-time chlorophyll-a monitoring was measured at 680 nm for the optical fluorescence detection of *C. reinhardtii*. Figure 2 shows the corrected fluorescence LiDAR peak signals of *C. reinhardtii* during the 16-day sampling period. The fluorescence LiDAR profile is the same as that of a previous study [28].

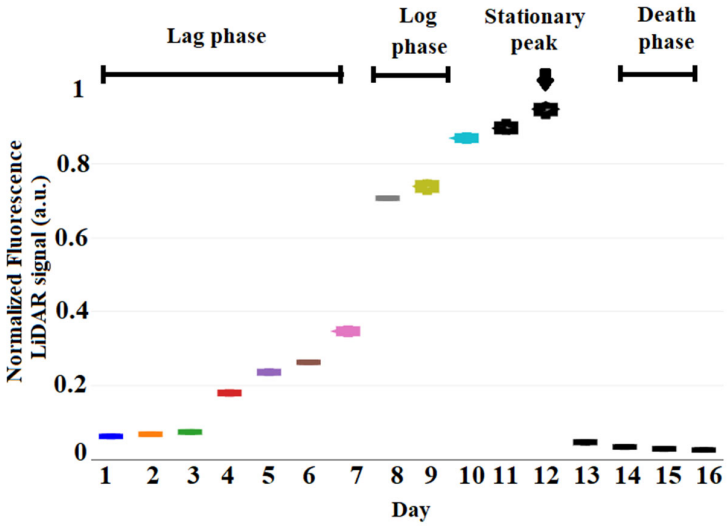

Figure 2. Normalized fluorescence LiDAR signal of *C. reinhardtii* during the 16-day sampling period. It shows a whisker and box plot showing the different growth phases of *C. reinhardtii*.

The 16-day sampling period showed the growth phases of *C. reinhardtii* from the lag phase to death phase. It was shown that the corrected fluorescence LiDAR signal profiles of *C. reinhardtii* exhibited a maximum value at the optical range of 5.7 m. The noise measurements showed minimum values ranging from 0 to 18 photon counts. The normalized fluorescence LiDAR signal was measured in arbitrary units (a.u.). The lag phase started from Day 1 to Day 7 with normalized fluorescence LiDAR signals ranging from 0.03 to 0.36 a.u. An increase from 0.67 to 0.91 a.u. shows the log phase from the 8th to 11th day. No stationary phase but a stationary peak was observed during Day 12 with a signal of 0.97 a.u. The death phase of *C. reinhardtii* started from Day 13 to Day 16, with the fluorescence LiDAR signal ranging from 0.02 to 0.1.

In this study, a time–range intensity profile of *C. reinhardtii* was created (Figure 3). The x-axis is the sampling days, y-axis is the optical range (in meters), and z-axis is the measured fluorescence signal (in a.u.).

The time–range intensity profile of *C. reinhardtii* shows the changes in the growth phases. The normalized fluorescence intensity scale ranges from 0 to 1. The range-resolved fluorescence LiDAR signal showed an increasing intensity from Day 1 to Day 12. As stated in the methodology, the beam pulse width is 1.2 m and the resolution is 0.5 m. This resolution causes an increasing fluorescence LiDAR intensity value before 5.7 m. The chlorophyll-a measurements after 5.7 m were affected by time delay, measured by the pulsed LED fluorescence LiDAR signal. This is due to an increase in concentration causing an increase in multiple scattering of the *C. reinhardtii* found from Day 9 to Day 12 [37].

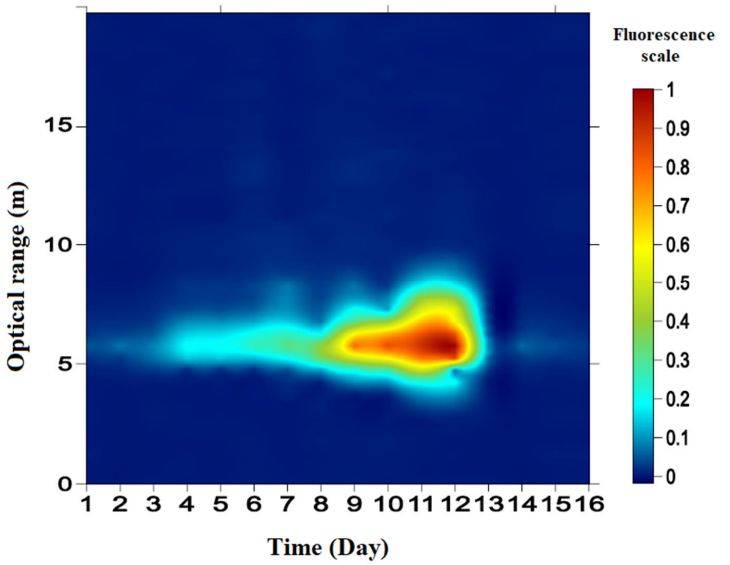

Figure 3. Time–range intensity profile of *C. reinhardtii* during the 16-day sampling period.

3.2. Optical Density and EEM Fluorescence Measurements

EEM shows the behavior of *C. reinhardtii*'s chlorophyll-a pigment from Day 1 to Day 16. This explains the excitation-emission pair ranging from 250 to 450 nm in excitation wavelength and 600 to 800 nm in emission (fluorescence) wavelength. It can be seen that the fluorescence spectroscopy measurements can also provide the growth dynamics of *C. reinhardtii*, as shown in Figure 4.

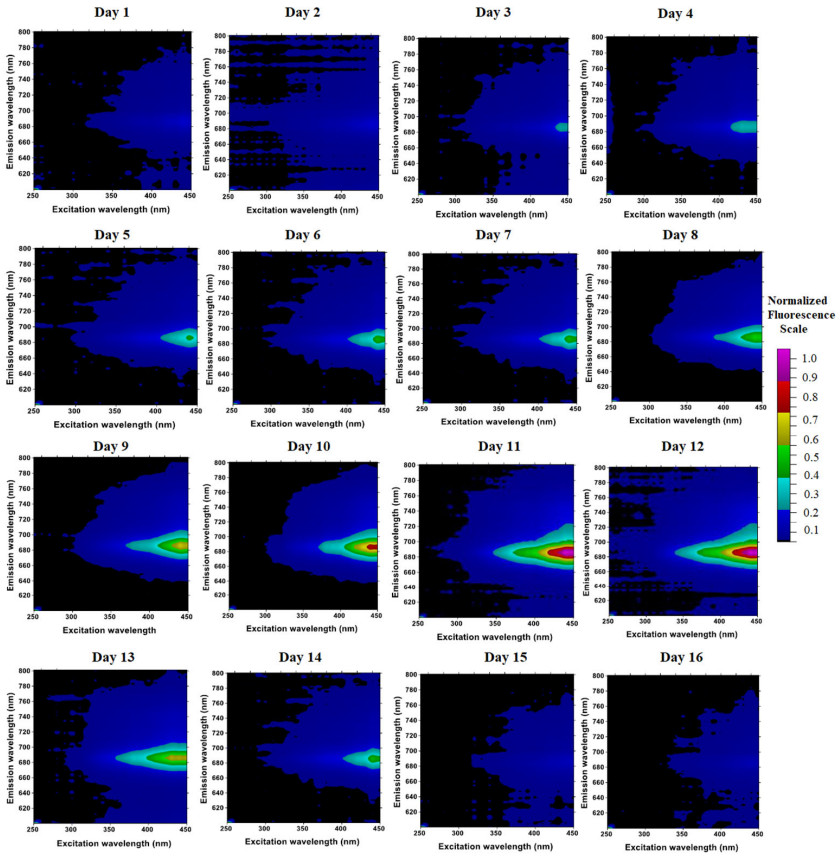

Figure 4. EEM measurements of *C. reinhardtii* during the 16-day sampling period. Single fluorescence peak was observed in each EEM.

The low-temperature fluorescence spectra were analyzed, showing different bands. As observed, *C. reinhardtii* exhibited a major peak range from 680 to 685 nm, which corresponds to protein complexes (LHCII and PSII core) [38]. Using two-way ANOVA, no significant differences were observed at OD650, OD680 and OD700; hence, an optical density at 680 nm was used for correlation between parameters [39]. Figure 5 shows the measured OD680 and peak signal from the EEM fluorescence of *C. reinhardtii*.

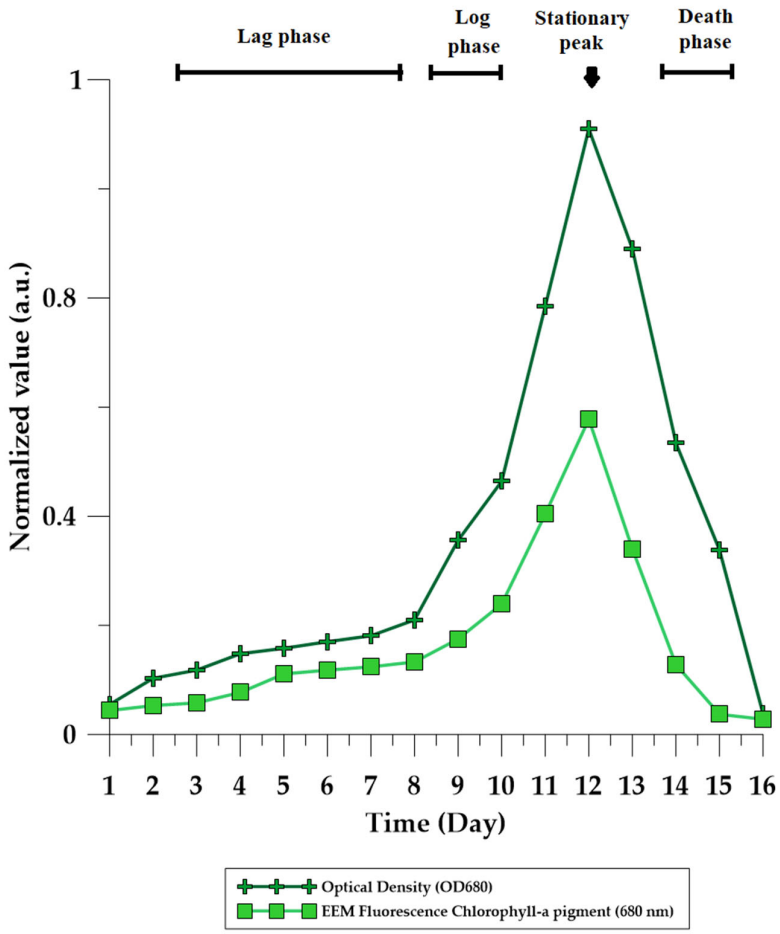

Figure 5. Optical density and EEM fluorescence measurements of *C. reinhardtii* at 680 nm. The growth phase of the algae is observable at specific cultivation parameters.

The chlorophyll-a concentration based on the two standard methods, namely optical density and EEM fluorescence chlorophyll-a measurements, shows the growth phases of *C. reinhardtii*. The same trend can be observed in the fluorescence LiDAR profile during the 16-day sampling period. A linear correlation was observed between the fluorescence LiDAR signal and the EEM fluorescence chlorophyll-a pigment, both measured at 680 nm. This trend was observed due to the similarity in the method performed as compared to the absorbance measurements at 680 nm.

3.3. Water Quality and Weather Observations

Water quality measurements are an important factor in understanding the growth behavior of any algal species [40,41]. We performed the remote sensing fluorescence LiDAR measurements of *C. reinhartdii* at nighttime (16:00–20:00). pH and water temperature were measured every after the fluorescence LiDAR measurements. Temperature and relative humidity were recorded by a weather station simultaneously. Figure 6 shows the water quality and weather parameters measured during the testing.

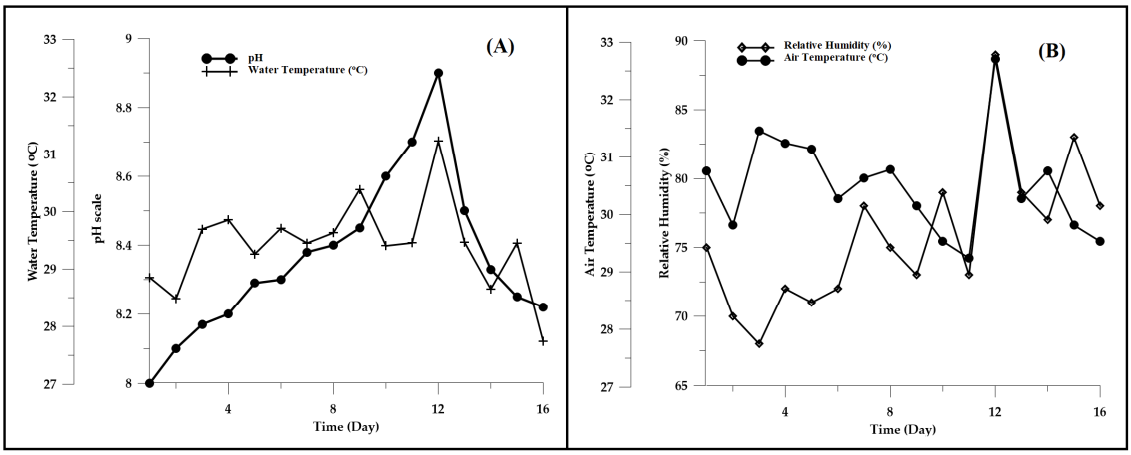

Figure 6. Line plots of (**A**) water quality parameters (water temperature and pH), and (**B**) weather measurements (air temperature and relative humidity) over the 16-day sampling period.

In this study, we have presented the impacts of water and weather parameters in the phases of *C. reinhardtii* [42]. The pH of *C. reinhardtii* was measured daily. Changes in pH exhibit an increasing trend from the lag phase to stationary peak. The maximum pH observed was found on Day 12 of cultivation, ranging from 8.7 to 8.9. The same trend was also observed for water temperature, which ranged from 28.04 to 31.56 °C. Relative humidity and air temperature were also recorded at the maximum value on Day 12 and suddenly decreased thereafter. This is due to the death of *C. reinhardtii*, as observed from the measurements conducted.

During the start of death phase, rotifers were observed and considered as predators of *C. reinhardtii* [43]. Rotifers are wheel animalcules that constitute the phylum Rotifera. Microalgae are considered as the food of rotifers, and this leads to the depletion of nutrients and growth of *C. reinhardtii* in the tank.

3.4. Correlation between Measurements

To further understand the relationships between parameters, Pearson's r linear correlation table was computed, as shown in Table 3. The mean and standard deviation were also included to determine the average values and the variation of the set of values provided. The *p*-value was measured to check the level of significance between two parameters.

Optical density and fluorescence measurements are the most convenient measurements of biomass concentration in microalgae analysis [44]. The estimated chlorophyll-a pigment of *C. reinhardtii* is as follows: OD680 (0.35 ± 0.32), EEM fluorescence chlorophyll pigment at 680 nm (0.17 ± 0.15), and measured fluorescence LiDAR peak value at 680 nm (0.38 ± 0.31).

The fluorescence LiDAR peak signal measurements indicated highly correlated values with OD680 (r = 0.77; *p*-value = 0.00049) and measured fluorescence chlorophyll-a pigment (r = 0.75; *p*-value = 0.0008). It also showed positive linear correlation with pH (r = 0.83; *p*-value = 0.00006) and water temperature (r = 0.63; *p*-value = 0.0089). It also showed the effects for water quality and weather parameters in the growth dynamics of microalgae.

Table 3. Statistical summary of all data collected from the *C. reinhardtii* cultivation.

N = 16	Mean/SD	Range-Resolved Fluorescence LiDAR Peak Value	OD680	EEM Chlorophyll-a Pigment (680 nm)	pH	Water Temp (°C)	Rel. Humidity (%)	Air Temp (°C)
Range-resolved fluorescence LiDAR peak value	0.38/0.31	1	0.00049 [a,b,c]	0.0008 [a,b,c]	0.00006 [a,b,c]	0.0089 [a,b,c]	0.2930	0.0211
OD680	0.35/0.32	0.77 *	1	0.00001 [a,b,c]	0.000019 [a,b,c]	0.035 [b,c]	0.01 [b,c]	0.48
EEM Chlorophyll-a pigment (680 nm)	0.17/0.15	0.75 *	0.93 *	1	0.00001 [a,b,c]	0.01 [a,b,c]	0.03 [b,c]	0.27
pH	8.36/0.23	0.83 *	0.86 *	0.93 *	1	0.012 [b,c]	0.021 [b,c]	0.61
Water temp (°C)	29.42/0.79	0.63 *	0.53 *	0.62 *	0.61 *	1	0.259	0.019 [b,c]
Rel Humidity (%)	75.75/5.30	0.28 *	0.62 *	0.54 *	0.57 *	0.30 *	1	0.435
Air temp (°C)	30.51/0.88	0.07 *	0.19 *	0.27 *	0.14 *	0.58 *	0.21 *	1

Statistically significant at (a) p <0.01, (b) p < 0.05, and (c) p < 0.10; * r-value.

4. Discussion

Our paper provides a real-time chlorophyll-a monitoring of *C. reinhardtii* using the portable LED fluorescence LiDAR system. The development of a non-contact, near-range fluorescence LiDAR system is important in areas wherein satellite systems cannot provide accurate data. This study provides new techniques for fluorescence LiDAR systems for environmental monitoring. Figures 2 and 3 show the fluorescence LiDAR signal of *C. reinhardtii* observed at specific cultivation parameters. As observed, the growth dynamics of *C. reinhardtii* are demonstrated from the lag phase to death phase. In estimating chlorophyll-a concentration, methods such as EEM fluorescence spectroscopy (Figure 4) and optical density (Figure 5) are commonly performed. The same trend was observed for the growth dynamics of *C. reinhardtii* using the standard methods and the fluorescence LiDAR signal.

The pulsed 385 nm LED module showed robustness with its high stability in optical power and wavelength (Table 2). It demonstrated its effectiveness in estimating the chlorophyll-a pigment of *C. reinhardtii* in near-range applications under controlled conditions. The optical transceiver of the LED LiDAR system is also stable because of the wider beam divergence and receiver's field of view (Table 2). In a controlled environment, water quality and weather (Figure 6) measurements were also observed to understand the growth behavior of *C. reinhardtii*. These measured parameters strongly supported our fluorescence LiDAR signal results in estimating chlorophyll-a. The cause of death of the algae is due to the changing water quality and weather parameters, which lead to the increase in rotifers. The gradual increase in pH and air and water temperatures in the algal tank showed a linear correlation with the observed fluorescence LiDAR signal of *C. reinhardtii*. Our results verified the feasibility of our fluorescence LiDAR system in monitoring the chlorophyll-a of any algal biomass.

Thus, it is a good alternative technique compared to standard methods for estimating chlorophyll-a pigment. The system can be further improved in terms of light intensity since it was only evaluated during nighttime conditions. Improvements in the sensing depth can also be an area of further study. Future studies could use laser diodes as the transmitting systems, which can be used for algal concentration monitoring using unmanned vehicles.

5. Conclusions

This is the first time, based on our research findings, that a portable light-emitting diode fluorescence LiDAR system using a pulsed LED module was used for real-time water quality assessment. It was verified experimentally that the observed fluorescence LiDAR signal can be used for approximating the chlorophyll-a concentration of *C. reinhardtii* in a controlled environment. This was supported by the positive correlation between the range-resolved fluorescence LiDAR signal and OD680 (r = 0.77; p = 0.00049) and EEM fluorescence

chlorophyll-a pigment at 680 nm (r = 0.75; p = 0.0008). It also showed a positive linear correlation with pH measurements (r = 0.83; p = 0.0006) and water temperature (r = 0.63; p = 0.0089). The system can clearly estimate the chlorophyll-a pigment of an algae from the lag phase to the death phase considering a specific cultivation parameter. There are several factors that can affect the estimated chlorophyll-a concentration, such as pH, temperature, and predators, which are proven in this study.

Author Contributions: Conceptualization, J.G.C., T.S., E.A.V. and M.C.D.G.; Methodology, J.G.C., Formal analysis, J.G.C., M.C.D.G.; Investigation, J.G.C. Writing—original draft preparation, J.G.C., T.S., E.A.V. and M.C.D.G. All authors have read and agreed to the published version of the manuscript.

Funding: This research received no external funding.

Institutional Review Board Statement: Not applicable.

Informed Consent Statement: Not applicable.

Data Availability Statement: Not applicable.

Acknowledgments: J.G. Cadondon acknowledges financial support from DOST ASTHRDP-NSC scholarship and UP Visayas. We would like to thank DLSU-URCO project No. 16 IR2TAY19-2TAY21 entitled "Water Quality and Fluorescence Measurements of Water Bodies". The researchers also acknowledge CENSER through EARTH lab of the De La Salle University for supporting this project.

Conflicts of Interest: The authors declare no conflict of interest.

References

1. Fields, F.J.; Lejzerowicz, F.; Schroeder, D.; Ngoi, S.M.; Tran, M.; McDonald, D.; Jiang, L.; Chang, J.T.; Knight, R.; Mayfield, S. Effects of the microalgae *Chlamydomonas* on gastrointestinal health. *J. Funct. Foods* **2020**, *65*, 103738. [CrossRef]
2. Matos, J.; Cardoso, C.; Bandarra, N.M.; Afonso, C. Microalgae as health ingredients for functional food: A review. *Food Funct.* **2017**, *8*, 2672–2685. [CrossRef] [PubMed]
3. Caporgno, M.P.; Mathys, A. Trends in microalgae incorporation into innovative food products with potential health benefits. *Front. Nutr.* **2018**, *5*, 58. [CrossRef] [PubMed]
4. Fallah, A.A.; Sarmast, E.; Habibian Dehkordi, S.; Engardeh, J.; Mahmoodnia, L.; Khaledifar, A.; Jafari, T. Effect of Chlorella supplementation on cardiovascular risk factors: A meta-analysis of randomized controlled trials. *Clin. Nutr.* **2018**, *37*, 1892–1901. [CrossRef]
5. Batista, A.P.; Gouveia, L.; Bandarra, N.M.; Franco, J.M.; Raymudo, A. Comparison of microalgal biomass profiles as novel functional ingredient for food products. *Algal Res.* **2013**, *2*, 164–173. [CrossRef]
6. Springer Nature. Chlamydomonas reinhardtii. 2019. Available online: https://www.nature.com/subjects/chlamydomonas-reinhardtii (accessed on 26 July 2022).
7. Scaife, M.A.; Nguyen, G.T.; Rico, J.; Lambert, D.; Helliwell, K.E.; Smith, A.G. Establishing *Chlamydomnas reinhardtii* as an industrial biotechnology host. *Plant J.* **2015**, *82*, 532–546. [CrossRef]
8. Harris, E.H. *Chlamydomonas* as a model organism. *Annu. Rev. Plant Physiol. Plant Mol. Biol.* **2001**, *52*, 97–112. [CrossRef]
9. Sommer, U.; Adrian, R.; De Senerpont Domis, L.; Elser, J.J.; Gaedke, U.; Ibeling, B.; Jeppesen, E.; Lurling, M.; Molinero, J.C.; Mooij, W.M.; et al. Beyond the plankton ecology group (PEG) model: Mechanism driving plankton succession. *Annu. Rev. Ecol. Evol. Syst.* **2012**, *43*, 429–448. [CrossRef]
10. Coleman, D.C.; Callaham, M.A., Jr.; Crossley, D.A., Jr. *Fundamental of Soil Ecology*, 3rd ed.; Academic Press: Cambridge, MA, USA, 2017.
11. Buysschaert, B.; Vermijs, L.; Naka, A.; Boon, N.; De Gusseme, B. Online flow cytometric monitoring of microbial water quality in full-scale water treatment plant. *Clean Water* **2018**, *1*, 16. [CrossRef]
12. Helmi, K.; David, F.; Di Matrino, P.; Jaffrezic, M.-P.; Ingrand, V. Assessment of flow cytometry for microbial water quality monitoring in cooling tower water and oxidizing treatment facility. *J. Microbiol. Methods* **2018**, *152*, 201–209. [CrossRef]
13. Cadondon, J.G.; Napal, J.P.D.; Abe, K.; De Lara, R.; Vallar, E.A.; Orbecido, A.H.; Belo, L.P.; Galvez, M.C.D. Characterization of water quality and fluorescence measurements of dissolved organic matter in Cabuyao river and its tributaries using excitation-emission matrix spectroscopy. *J. Phys. Conf. Ser.* **2020**, *1593*, 012033. [CrossRef]
14. Cadondon, J.G.; Vallar, E.A.; Belo, L.P.; Orbecido, A.H.; Galvez, M.C.D. UV-vis absorbance and fluorescence characterization of Pasig River surface water samples towards the development of an LED fluorescence lidar system. *Int. J. Adv. Sci. Eng. Inf. Technol.* **2021**, *11*, 968–980. [CrossRef]
15. Stedmon, C.A.; Bro, R. Characterizing dissolved organic matter fluorescence with parallel factor analysis: A tutorial. *Limnol. Oceanogr. Methods* **2008**, *6*, 572–579. [CrossRef]

16. Coble, P.; Lead, J.; Baker, A.; Reynolds, D.; Spencer, R. *Aquatic Organic Matter Fluorescence*; Cambridge Environmental Chemistry Series; Cambridge University Press: Cambridge, UK, 2014.
17. Fellman, J.B.; Hood, E.; Spencer, R.G.M. Fluorescence spectroscopy opens new windows into dissolved organic matter dynamics in freshwater ecosystems: A review. *Limnol. Oceanogr.* **2010**, *55*, 2452–2462. [CrossRef]
18. Campbell, J.B.; Wynne, R.H. *Introduction to Remote Sensing*, 5th ed.; Guilford Press: New York, NY, USA, 2011.
19. Rantajarvi, E.; Olsonen, R.; Hallfors Leppanen, J.-M.; Raateja, M. Effect of sampling frequency on detection of natural variability in phytoplankton: Unattended high-frequency measurements on board ferries in the Baltic Sea. *ICES J. Mar. Sci.* **1998**, *55*, 697–704. [CrossRef]
20. Boss, E.; Haentjens, N.; Ackleson, S.G.; Balch, B.; Chase, A.; Dall'Olmo, G.; Freeman, S.; Liu, Y.; Loftin, J.; Neary, W.; et al. Inherent optical property measurements and protocols: Best practices for the collection and processing of ship-based underway flow-through optical data. In *Ocean Optics & Biogeochemistry Protocols for Satellite Ocean Colour Sensor Validation*; IOCCG Protocol Series; Neeley, A.R., Mannino, A., Eds.; IOCCG: Darmouth, NS, Canada, 2019; Volume 4.0.
21. Li, Y.; Yu, K.; Zhang, W.; Li, D.; Zhao, Z.; Jiang, X.; Jin, D.; Shang, B.; Wang, H. Progress of airborne lidar of ocean chlorophyll observations including algorithms and instruments. *IOP Conf. Ser. Mater. Sci. Eng.* **2020**, *730*, 012046. [CrossRef]
22. Yoder, J.A.; Aiken, J.; Swift, R.N.; Hoge, F.E.; Stegmann, P.M. Spatial variability in near surface chlorophyll-a fluorescence measured by the Airborne Oceanographic Lidar (AOL). *Deep. Se Res. Part II Tp. Stud. Oceanogr.* **1993**, *40*, 37–53. [CrossRef]
23. Papenfus, M.; Schaeffer, B.; Pollard, A.I.; Loftin, K. Exploring the potential value of satellite remote sensing to monitor chlorophyll-a for US lakes and reservoirs. *Environ. Monit. Assess.* **2020**, *192*, 808. [CrossRef]
24. Topp, S.N.; Pavelsky, T.M.; Jensen, D.; Simard, M.; Ros, M.R.V. Research trends in the use of remote sensing for inland water quality science: Moving towards multidisciplinary. *Water* **2019**, *12*, 169. [CrossRef]
25. Raimondi, V.; Cecchi, G.; Lognoli, D.; Palombi, L.; Gronlund, R.; Johansson, A.; Svanberg, S.; Barup, K.; Hallstrom, J. The fluorescence lidar technique for the remote sensing of photoautotrophic biodeteriogens in the outdoor cultural heritage: A decade of in situ experiments. *Inter. Biodeterior. Biodegrad.* **2009**, *63*, 823–835. [CrossRef]
26. Saito, Y.; Takano, K.; Kobayashi, F.; Kobayashi, K.; Prk, H.-D. Development of a UV laser-induced fluorescence for monitoring blue-green algae in Lake Suwa. *Appl. Opt.* **2014**, *53*, 7030–7036. [CrossRef] [PubMed]
27. Palmer, S.C.; Pelevin, V.V.; Goncharenko, I.; Kovacs, A.W.; Zlinsky, A.; Presing, M.; Horvath, H.; Nicolas-Pera, V.; Balzier, H.; Toth, V.R. Ultraviolet fluorescence LiDAR (UFL) as a measurement tool for water quality parameters in Turbid Lake conditions. *Remote Sens.* **2013**, *5*, 4405–4422. [CrossRef]
28. Cadondon, J.G.; Ong, P.M.B.; Vallar, E.A.; Shiina, T.; Galvez, M.C.D. Chlorophyll-a pigment measurement of spirulina in algal growth monitoring using portable pulsed LED fluorescence lidar system. *Sensors* **2022**, *22*, 2940. [CrossRef] [PubMed]
29. Saito, Y.; Ichihara, K.; Morishita, K.; Uchiyama, K.; Kobayashi, F.; Tomida, T. Remote detection of the fluorescence spectrum of natural pollens floating in the atmosphere using a laser-induced-fluorescence spectrum (LIPS) Lidar. *Remote Sens.* **2018**, *10*, 1533. [CrossRef]
30. Shiina, T. LED mini lidar for atmospheric application. *Sensors* **2019**, *19*, 569. [CrossRef]
31. Koyama, M.; Shiina, T. Light source module for LED mini-lidar. *Rev. Laser Eng.* **2011**, *39*, 617–621. [CrossRef]
32. Ong, P.M.B.; Shiina, T.; Manago, N.; Kuze, H.; Senshu, H.; Otobe, N.; Hashimoto, G.; Kawabata, Y. A compact LED Lidar system fitted for a mars rover—Design and ground experiment. *EPJ Web Conf.* **2018**, *176*, 02013. [CrossRef]
33. Stanier, R.Y.; Kunisawa, R.; Mandel, M.; Cohen-Bazire, G. Purification and properties of unicellular blue-green algae (Order Chroococcales). *Bacteriol. Rev.* **1971**, *35*, 171–205. [CrossRef]
34. Measures, R. *Laser Remote Sensing*; Wiley Publishing: Hoboken, NJ, USA, 1984.
35. Janssen, P.J.D.; Laambreva, M.D.; Plumere, N.; Bartolucci, C.; Antonacci, A.; Buonasera, K.; Frese, R.N.; Scognamiglio, V.; Rea, G. Photosynthesis at the forefront of a sustainable life. *Front. Chem.* **2014**, *2*, 36. [CrossRef]
36. Donohue, J.M. Water conditioning, industrial. In *Encyclopedia of Physical Science and Technology*, 3rd ed.; Elsevier: Amsterdam, The Netherlands, 2003; pp. 671–697. [CrossRef]
37. Miller, S.D.; Stephens, G.L. Multiple scattering effects in the lidar pulse stretching problem. *J. Geophys. Res.* **1999**, *104*, 22205–22219. [CrossRef]
38. Kalra, I.; Wang, X.; Cvetkovska, M.; Jeong, J.; McHargue, W.; Zhang, R.; Huner, N.; Yuan, J.S.; Morgan-Kiss, R. *Chlamydomonas* sp. UWO 241 exhibits high cyclic electron flow and rewired metabolism under high salinity. *Plant Physiol.* **2020**, *183*, 588–601. [CrossRef]
39. Young, E.B.; Reed, L.B.J.A. Growth Parameters and responses of green algae across a gradient of phototrophic, mixotrophic and heterotrophic conditions. *Peer J* **2022**, *10*, e13776. [CrossRef]
40. Omar, W.M. Perspectives on the use of algae as biological indicators for monitoring and protecting aquatic environments, with special reference to Malaysian freshwater ecosystems. *Trop. Life Sci. Res.* **2010**, *21*, 51–67.
41. Stevenson, J. Ecological assessments with algae: A review and synthesis. *J. Phycol.* **2014**, *50*, 437–461. [CrossRef]
42. Krishnan, V.; Uemura, Y.; Thanh, N.T.; Khalid, N.A.; Osman, N.; Mansor, N. Three types of marine microalgae and *Nannocholoropsis oculate* cultivation for potential source of biomass production. *J. Phys. Conf. Ser.* **2015**, *622*, 012034. [CrossRef]

43. Lurling, M.; Beekman, W. Palmelloids formation in *Chlamydomonas reinhardtii*: Defense against rotifer predators? *Ann. Limnol. Int. J. Limnol.* **2006**, *42*, 65–72. [CrossRef]
44. Schagerl, M.; Siedler, R.; Konopacova, E.; Ali, S.S. Estimating biomass and vitality of microalgae for monitoring cultures: A roadmap for reliable measurements. *Cells* **2022**, *11*, 2455. [CrossRef]